O.U. Velasco Fuentes and G.J.F. van Heijst

Laboratory Experiments on Dipolar Vortices in a Rotating Fluid

Abstract

The behaviour of dipolar vortices on a β-plane is investigated in the laboratory using a rotating fluid with a varying depth. Dipoles initially directed under a certain angle relative to the west-east axis showed meandering or cycloid-like trajectories. For East-travelling dipoles (ETD's) a small deviation from zonal motion results in small oscillations around the equilibrium latitude. For West-travelling dipoles (WTD's) small deviations result in large displacements in meridional direction. ETD's increase in size and eventually split into two independent monopoles.

Introduction

Large scale motions in the oceans and in the atmosphere, being two-dimensional in a first approximation, are characterized by the emergence of coherent vortices. After the monopolar vortex the dipole is the most commonly occurring vortex structure. The dipolar vortex has two remarkable properties: it possesses a separatrix and it has a non-zero linear momentum. Therefore this vortex structure provides an efficient mechanism for the transport of mass and momentum over large distances. In particular, oceanic dipolar vortices are believed to play an important role in the transport of scalar properties such as heat, salt, nutrients and other biochemical components.

The dynamics of geophysical flows is further influenced by the gradient of the Coriolis parameter in the latitudinal direction, usually referred to as the β-effect. A similar gradient of the ambient vorticity can be caused by variations of the depth of the fluid. When these variations are linear and small, the result is equivalent to a gradient of the Coriolis parameter (with the direction of steepest bottom slope corresponding with the northern direction). This effect is sometimes called "topographic β-effect".

There are several dipolar solutions, also called modons, which can exist in such inhomogeneous media (see Flierl, 1987). One common characteristic of these modons is that they are either stationary or they translate steadily along lines of equal ambient vorticity. An important question concerns the existence of similar structures that propagate transversally to these isolines.

One approach to this problem has been the representation of the dipole by a couple of point vortices. During the evolution the relative circulation changes to preserve potential vorticity. Kawano and Yamagata (1977) first found three "regimes" in the motion of the couples: i) eastward meandering, ii) westward cycloid-like trajectories, and iii) the "non-propagating" mode, in which the couple moves along an 8-shaped curve fixed in space. Zabusky and McWilliams (1982) presented calculations of a point-vortex couple and a dipole represented by two pairs of point vortices. These point-vortex calculations showed good agreement with numerical simulations of a modon solution for the first oscillation.

Makino *et al.* (1981) used "tilted" modons as initial conditions for numerical simulations. They found that the modons survive as coherent structures, moving along meandering trajectories in eastward direction or along cycloid-like paths in westward direction, depending on the tilting angle. Using a perturbation technique, Nycander and Isichenko (1990) also found these two regimes as well as the "non-propagating" mode. They also showed that the decay due to generation of relative vorticity was negligible during one oscillation of the dipole.

The results reported here concern flow measurements and visualizations of the evolution of dipoles propagating transversally to the lines of equal ambient vorticity.

Point-vortex model

On a β-plane every column of fluid is assumed to conserve potential vorticity during the evolution, i.e. $q = \omega + \beta y$ is constant, where ω is the relative vorticity and β is the gradient of ambient vorticity in the northern direction y. On a rotating sphere $\beta = 2\Omega \cos \phi_0 / R$, with Ω the angular velocity, ϕ_0 a reference latitude and R the sphere's radius. On a "topographic β-plane" $\beta = 2\Omega s / h_0$, with s the gradient of the fluid depth and h_0 the reference depth.

This principle can be implemented in the point-vortex model under the assumption that a point vortex represents a small patch (with area πL^2) of uniform vorticity $\bar{\omega}$. Using conservation of potential vorticity, the point-vortex's circulation ($\kappa = \bar{\omega} \pi L^2$) can be expressed as a function of the position:

$$\kappa = \kappa_0 + \pi L^2 \beta (y_0 - y)$$

where y_0 represents the initial latitude, at which the vortex has strength κ_0.

The motion of a point-vortex dipole on the β-plane can be described by a couple of ordinary differential equations (see e.g. Velasco Fuentes and van Heijst, 1994). In the case of a weak β (more precisely $\beta d L^2 / \kappa_0 \ll 1$, with d the distance between the point-vortices) the evolution is described by:

$$\frac{d^2 \alpha}{dt^2} + \frac{L}{d} \beta U \sin \alpha = 0$$

where α is the angle of the dipole's velocity vector with respect to the lines of equal ambient vorticity and $U = \kappa_0/2\pi d$ is the initial translation velocity of the dipole. Initial conditions are $\alpha'(0) = 0$ and $\alpha(0) = \alpha_0$.

This equaton is identical to the simple pendulum equation and can be solved in terms of elliptical integrals. The condition $\alpha'(0) = 0$ ensures that all the solutions represent oscillations in the dipole's direction of propagation. The stability properties of the dipole trajectory can be immediately established: an ETD ($\alpha_0 = 0$) performs small oscillations when its trajectory is perturbed, whereas any small perturbation causes the WTD ($\alpha_0 = \pi$) to make a big loop.

Experimental arrangement

The experiments were carried out in a rectangular tank of horizontal dimensions $100 \times 150\ \text{cm}^2$ and 30 cm depth mounted on a rotating table. In most experiments the angular speed of the system was $\Omega = 0.56\ \text{s}^{-1}$, so that the Coriolis parameter $f = 1.12\ \text{s}^{-1}$. The working depth of the fluid was varied from 15 to 20 cm, and a false bottom was raised 4 to 8 cm along one of the long sides to provide the topographic β-effect. With these parameter settings the equivalent value of β measured approximately $0.25\ \text{m}^{-1}\ \text{s}^{-1}$.

Once the fluid was in solid body rotation a columnar dipole vortex was generated by slowly moving a small, bottomless cylinder of 8 cm diameter horizontally along a straight line relative to the rotating tank, while slowly lifting it out of the fluid. The vorticity generated by the motion of the cylinder accumulates in a dipolar structure in the wake of the cylinder. After typically 1–2 rotation periods the organization of the vortex flow is completed. The Rossby number for the resultant dipolar structure, defined as $R_O = U/2\Omega r$ with U as the maximal velocity and r as the radius of the dipole, is of order 0.1 to 0.2.

In a first series of experiments dye was added to the fluid within the small cylinder before generating the dipole. Photographs of the evolving dipole were taken at intervals of typically 5 to 15 sec by a camera mounted in the rotating frame about 150 cm above the free surface of the fluid.

Flow measurements were made from photographic streaks of small (1 mm diameter) paper particles floating on the free surface. The velocity field is measured from the lengths and orientations of particle streaks. Then the velocity field is interpolated onto a regular grid using cubic splines. The relative vorticity ($\omega = v_x - u_y$) is calculated analytically from the interpolating polynomials and the stream function is obtained by numerically inverting the Poisson equation $\nabla^2\psi = -\omega$.

Meandering dipoles

A typical trajectory of a dipole initially moving towards shallower parts of the tank ("north") is shown in Figure 1a. In this case the dipole was initially directed

at some angle to the topography gradient, approximately to the "north-east". Due to the background rotation the two dipole halves experience asymmetric effects: the cyclonic vortex becomes weaker while the anticyclonic one becomes stronger, resulting in a trajectory curved in clockwise sense. The clockwise rotation brings the dipole southwards, and the asymmetry gradually diminishes. The dipole recovers its zero net circulation when it crosses the equilibrium line (where the height of the fluid column is equal to its initial value). Because of its own momentum the dipole moves further into deeper regions ("south"), so that the column of fluid is stretched further. Owing to this stretching, the cyclonic half becomes stronger and as a result the dipole's trajectory curves in anti-clockwise sense. After reaching its southernmost position the dipole moves back to its equilibrium latitude. At this stage the dipole has decayed and its propagation speed is reduced to almost zero.

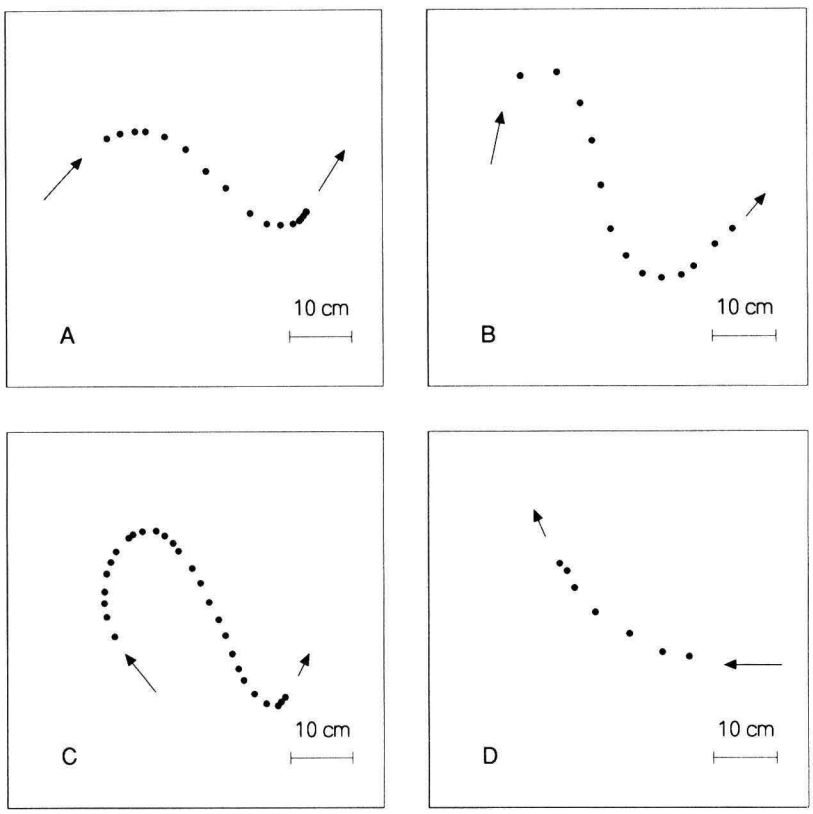

Fig. 1. Observed dipole trajectories for different initial direction of propagation: (A) northeast, (B) north, (C) northwest, and (D) west. The arrows indicate initial and final directions of the observed dipole translation. Since the medium depth h_0 of the fluid in the dipole evolution varies from one experiment to another (in the range 15 to 18 cm) the β-effect changes accordingly in the range 0.25–0.3 $m^{-1} s^{-1}$.

This squeezing and stretching mechanism is active for every initial orientation of the dipole axis. However, its effect is very different on dipoles moving initially at angles greater than $\pi/2$ (i.e. dipoles with a westward component in their motion) and on dipoles moving at angles smaller than $\pi/2$ (dipoles with an eastward component). When the initial angle is less than $\pi/2$ the dipole acquires

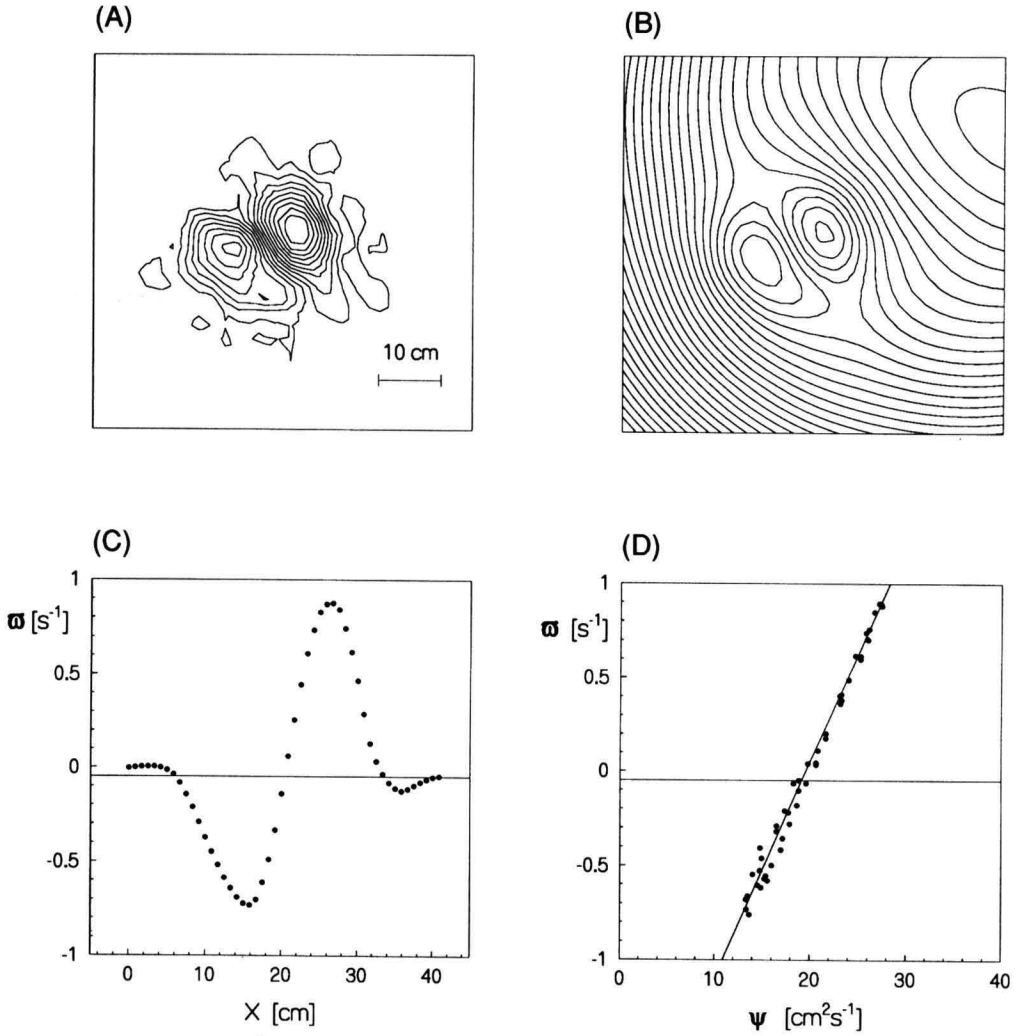

Fig. 2. Measured flow characteristics of a dipolar vortex on a β-plane at $t = 1.77T$, with $T = 11.3$ s the rotation period of the turntable. The dipole moved initially to the south and subsequently described a meandering path. The graphs represent (a) vorticity contours (contour interval CI $= 0.1\ s^{-1}$), (b) stream function contours (CI $= 2\ cm^2\ s^{-1}$) corrected for the observed motion of the dipole, (c) distribution of vorticity along a line crossing the points of extremal vorticity values and (d) ω-ψ relation, obtained by plotting the vorticity value against the stream function value of every grid point in the interior of the dipole. Experimental parameters: $f = 1.11\ s^{-1}$, $h_0 = 0.17$ m, $s = 0.23$, $\beta = 0.26\ m^{-1}\ s^{-1}$.

an asymmetry of the proper sign to pull it back to its equilibrium latitude. The smooth oscillation of a dipole with initial north-east motion appears in Figure 1a, and a similar trajectory can be seen in Figure 1b for a dipole released in northward direction. Dipoles with tilting angles greater than $\pi/2$ move initially away from the equilibrium latitude along a big loop before finally returning to it (see Figure 1c for an example of a dipole initially moving north-westward). Figure 1d shows an example of the trajectory instability of a West-travelling dipole (WTD). In this case the dipole moves northward and breaks up before being able to return to its initial latitude.

Flow measurements were done in the case of a dipole initially directed southward. When it reaches a mature state at time $t = 1.77$ (in units of the rotation period $T = 11.3$ s), the dipole moves in an approximate south-east direction. The cyclonic half is stronger, resulting in an anti-clockwise deflection of the dipole's trajectory. The density of the vorticity and stream function contours in Figures 2a,b shows a clear asymmetry between the two dipole halves. The centre of the dipole's rotational motion at this stage is also visible in the upper right corner of Figure 2b (note that both vorticity and stream function have been corrected for the motion of the dipole).

A remarkable feature in the cross-section of vorticity is the presence of a small ring of oppositely-signed vorticity around the dipole (see e.g. the small humps in the vorticity cross-section, Figure 2c). The shielding ring is caused by the advection of ambient fluid in meridional direction and leads to a widening of the dipole. At the earlier stages of the dipole motion the vortex structure was found to be characterized by a linear relation between ω and ψ, see Figure 2d. As a result of entrainment of passive fluid, at later stages a weak nonlinearity in the ω-ψ relation is developed.

Break-up of an ETD

Besides the asymmetry of stability properties a few more differences were observed between eastward and westward travelling dipoles. The ETD's were always larger and slower than the WTD's, which were compact and travelled relatively fast. These different types of behaviour can be explained by the secondary vorticity field generated in the fluid exterior to the vortex dipole (Velasco Fuentes and van Heijst, 1994). The magnitude of the secondary vorticity is of order βr, where r is the radius of the dipole. As β is increased the value of the generated vorticity gets closer to the values of the dipole's vorticity itself, thus producing a faster growth and eventually a break-up of the ETD. In the WTD the tendency to become compact and fast vanishes rapidly due to the instability of the westward trajectory.

In order to investigate the splitting of an ETD in more detail, an experiment was carried out using a strong β-effect ($\beta = 0.52\ \mathrm{m^{-1}\,s^{-1}}$). The formation of the dipolar structure was completed approximately 4–5 revolution periods after the lifting of the generating cylinder. In comparison with the previously shown

dipole (Figure 2), the size of the dipolar vortex was relatively large in this case, and the two halves were not compactly attached as before. At a later stage ($t = 14.5$) the separation between the two halves had increased significantly (Figures 3a,b) and a weak *westward* drift of the two halves was observed.

The vorticity distribution along the line joining the vortex centres (Figure 3c) shows an almost complete break-up of the dipole and it resembles that of two

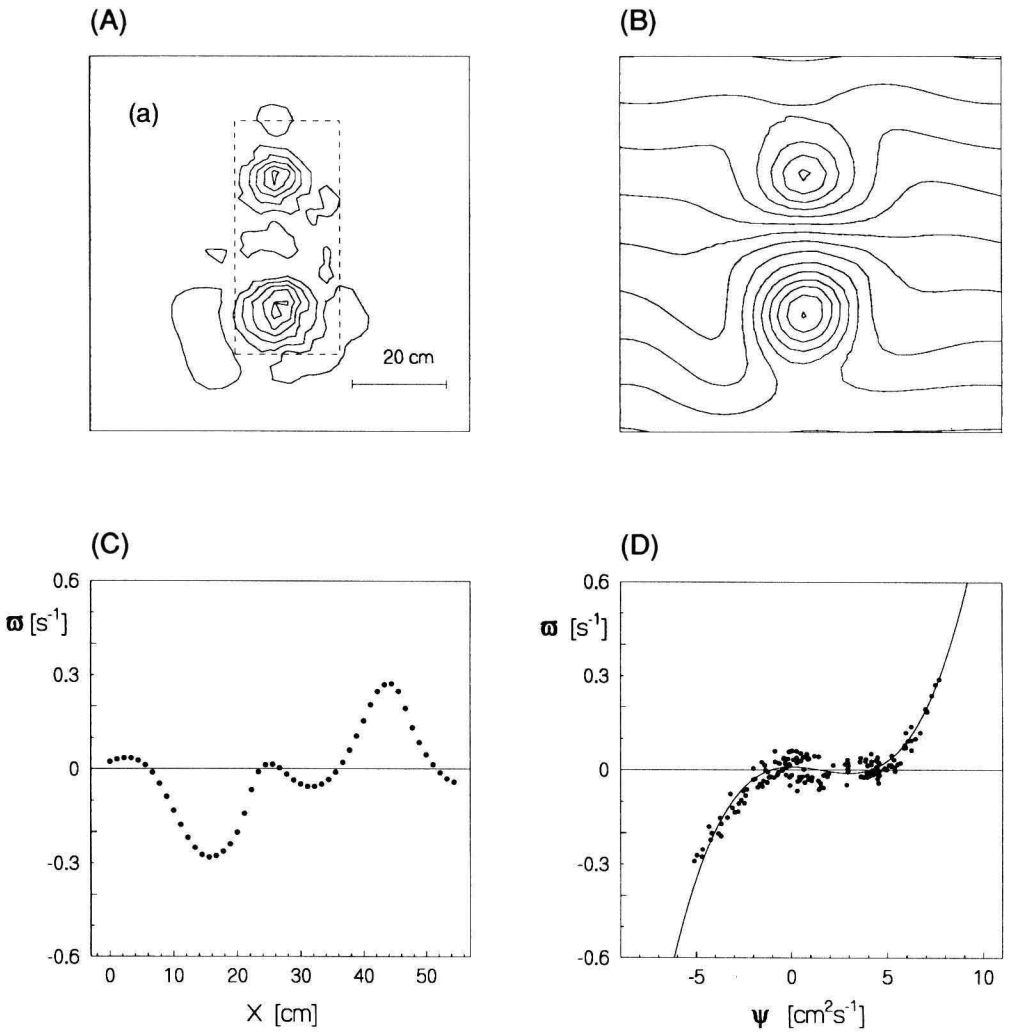

Fig. 3. Measured flow characteristics of the ETD after the splitting has been completed (at time t = 14.5 T): (a) vorticity contours (CI = 0.06 s^{-1}), (b) stream function contours (CI = 1 $cm^2\ s^{-1}$) corrected for the observed westward motion of the monopolar vortices, (c) vorticity distribution along a line intersecting the points of extremal vorticity, and (d) the ω-ψ plot obtained from the grid points in the rectangular area indicated by the broken line in (a). Experimental parameters: $f_0 = 1.1\ s^{-1}$, $h_0 = 0.16$ m, $s = 0.42$, $\beta = 0.52\ m^{-1}\ s^{-1}$.

(oppositely signed) isolated monopolar vortices placed close together (see e.g. Kloosterziel and van Heijst, 1992). The ω-ψ relation shows two antisymmetric branches which are reasonably approximated by a cubic polynomial (Figure 3d). Comparison with the ω-ψ relationship of an isolated monopolar vortex (e.g. van Heijst *et al.*, 1991), confirms that the ω-ψ plot in Figure 3d indeed represents a combination of a cyclonic and an anticyclonic shielded monopolar vortex. The considerable scatter can be attributed to the different meridional drift components of the vortices (which can not be simultaneously corrected for), and also to the non-steadiness of the individual vortices: as shown by e.g. Carnevale *et al.* (1991), the shielded monopolar vortex on a β-plane is not quasi-stationary, and loses vorticity while drifting.

Conclusions

In a series of dye experiments dipoles were initiated at different angles with respect of the isobaths. The trajectories of dipoles with an eastward component in their motion are in good agreement with theoretical predictions (Kawano and Yamagata, 1977; Makino *et al.*, 1981). Dipoles with a westward component agree only in the perturbation enhancement mechanism but do not show the 8-shaped path or the cycloid-like mode.

Flow measurements show variations of the relative vorticity that are in qualitative agreement with the predictions of the point-vortex model and numerical calculations. A functional relation is observed between vorticity and stream function, being linear at the first stages and becoming nonlinear at later stages.

Generation of relative vorticity by advection of ambient fluid in meridional direction causes ETD's to grow and to translate slower, while WTD's become compact and fast-moving during the first stages (before the development of the trajectory instability). The rate of growth of the ETD is determined by the gradient of ambient vorticity (β). A strong β-effect leads to the break-up of the ETD. After the separation of the dipole into two monopolar vortices, each vortex drifts independently under the β-plane dynamics, namely: the cyclonic half moves in northwestern direction and the anticyclonic vortex travels to the southwest.

Acknowledgement

O.U.V.F. gratefully acknowledges financial support from the Stichting voor Fundamenteel Onderzoek der Materie (FOM).

References

Carnevale, G.F., R.C. Kloosterziel & G.J.F. van Heijst, 1991 - Propagation of barotropic vortices over topography in a rotating tank. *J. Fluid Mech.* **233**, 119–139.

Flierl, G.R., 1987 - Isolated eddy models in geophysics. *Ann. Rev. Fluid Mech.* **194**, 93–530.

van Heijst, G.J.F., R.C. Kloosterziel & C.W.M. Williams, 1991 - Laboratory experiments on the tripolar vortex in a rotating fluid. *J. Fluid Mech.* **225**, 301–331.

Kloosterziel, R.C. & G.J.F. van Heijst, 1992 - The evolution of stable barotropic vortices in a rotating free-surface fluid. *J. Fluid Mech.* **239**, 607–629.

Kawano, J. & T. Yamagata, 1977 - The behaviour of a vortex pair on the beta plane. *Proc. Oceanogr. Soc. Japan* **36**, 83–84 (in Japanese).

Makino, M., T. Kamimura & T. Taniuti, 1981 - Dynamics of two-dimensional solitary vortices in a low-β plasma with convective motion. *J. Phys. Soc. Japan* **50**, 980–989.

Nycander, J. & M.B. Isichenko, 1990 - Motion of dipole vortices in a weakly inhomogeneous medium and related convective transport. *Phys. Fluids* **B2**, 2042–2047.

Velasco Fuentes, O.U. & G.J.F. van Heijst, 1994 - Experimental study of dipolar vortices on a topographic β-plane. *J. Fluid Mech.* **259**, 79–106.

Zabusky, N.J. & J.C. McWilliams, 1982 - A modulated point-vortex model for geostrophic, β-plane dynamics. *Phys. Fluids* **25**, 2175–2182.

Fluid Dynamics Laboratory
Eindhoven University of Technology
P.O. Box 513
5600 MB Eindhoven
The Netherlands